Chemiluminescence of argon bromide. I. The emission spectrum of ArBr

Michael F. Golde and Agust Kvaran

Citation: The Journal of Chemical Physics **72**, 434 (1980); doi: 10.1063/1.438869
View online: http://dx.doi.org/10.1063/1.438869
View Table of Contents: http://scitation.aip.org/content/aip/journal/jcp/72/1?ver=pdfcov
Published by the AIP Publishing

Chemiluminescence of argon bromide. I. The emission spectrum of ArBr

Michael F. Golde and Agust Kvaran[a)]

Department of Chemistry, University of Pittsburgh, Pittsburgh, Pennsylvania 15260
(Received 22 June 1979; accepted 25 September 1979)

In this first systematic study of the ArBr molecule, chemiluminescence spectra are generated by the reactions of metastable argon atoms with bromine-containing compounds. Three continua, due to the $B(1/2) - X(1/2)$, $B(1/2) - A(1/2)$ and $C(3/2) - A(3/2)$ transitions are characterized, their pressure dependences examined, and the extent of their overlap discussed in some detail. From the temperature dependence of the spectra, an upper limit for the electronic energy of the $B(1/2)$ state is derived: $T_{eB} \leq 61\,850\ \mathrm{cm}^{-1}$.

I. INTRODUCTION

The recent discovery of the diatomic noble-gas halides, formed in reactions of excited Ar, Kr, and Xe atoms with halogen-containing compounds,[1,2] has provided new insight into the mechanism of the extremely efficient quenching of excited noble-gas atoms,[3,4] has brought a new chemical perspective to the analogy between excited noble-gas atoms and ground state alkali atoms, and has led to the development of noble-gas halide lasers.

However, despite these applications, the structure and properties of the noble-gas halides themselves are still poorly understood at the experimental level. The reason is that, although these molecules have stable excited electronic states, they are largely unbound in their ground states. Thus, potential curves can only be derived from electronic spectroscopy and molecular beam elastic scattering experiments. The latter[5] has not yet proven very informative because the scattering involves more than one potential. Apart from emission spectra from low vibrational levels of the excited states of XeF and XeCl, which exhibit band structure,[6,7] the spectra are continuous and thus considerably less amenable to analysis.

Such an analysis must be based on, firstly, the absolute wavelength range occupied by the spectra and, secondly, the diffuse structure in the spectra, which reflect distinct contributions from different vibronic emitting states and also quantum mechanical interference effects in the overlap of the upper- and lower-state wave functions. The first semiclassical analysis,[8] carried out by one of the authors, merely established the importance of these factors in giving information about the potential curves involved, particularly the emitting state.

Complete simulations of the experimental spectra have been performed by Tellinghuisen *et al.*[9] and Setser and Tamagake.[10] In the former study of high-pressure spectra of the $B(\frac{1}{2})-X(\frac{1}{2})$ transitions of KrF, XeBr, and XeI, Boltzmann vibrational distributions were assumed for the emitting $B(\frac{1}{2})$ state. The analysis yielded potential curves and the r dependence of the electronic transition moment $\mu(r)$. Setser and Tamagake[10] analyzed the $B-X$ and $C(\frac{3}{2})-A(\frac{3}{2})$ continua of KrF at low pressure (about 1 Torr) using *ab initio* calculated potential curves[11] and the results of the high pressure study. Their principal findings were the vibrational distributions in the emitting states.

In the present papers, we examine emission spectra of ArBr at low pressure. For this molecule, no *ab initio* calculations of the potential curves have been published. Yet, as we shall attempt to establish, rather reliable spectral information can be derived. In this paper, the experimental chemiluminescence spectra arising from the reactions of excited Ar atoms with several Br-containing compounds are presented. The dynamics of the formation reactions are compared with those of the alkali atoms with similar reagents. In the following paper (Paper II), the analysis of the spectra is presented.

II. EXPERIMENTAL

The spectra were generated by the reactions of metastable electronically excited Ar atoms, $Ar(^3P_{0,2})$ with HBr, DBr, CH_2Br_2, Br_2, CF_3Br, CBr_4, and PBr_3 in a discharge–flow system, employing a weak dc discharge, as described previously.[12] The bulk carrier gas was Ar at a total pressure of between 0.5 and 4 Torr. The reagent gas accounted for typically 0.1%–1% of the total flow, the form of the spectrum being independent of reagent concentration. For some experiments, the observation vessel was cooled with dry ice, reducing the gas temperature typically to 240 K, as measured with a thermocouple.

Emission from the mixing zone of the reagents was detected using a vacuum monochromator and photomultipliers. For experiments performed at the University of Edinburgh, a Hilger 766 1-m normal incidence monochromator (kindly loaned by Dr. Robert Donovan) was used, with an EMR 542G photomultiplier, covering the spectral range 105–180 nm. The same region was covered at the University of Pittsburgh using a Minuteman 305MV 0.5 m Czerny-Turner monochromator; an EMI 9789 Q photomultiplier was also used, for observations in the region 160–500 nm. The emission spectra are characterized by strong atomic Br lines at wavelengths at and below 157.7 nm and relatively weak ArBr

[a)] Also: Department of Chemistry, University of Edinburgh, Edinburgh, EH9 3JJ, United Kingdom.

 0021-9606/80/010434-08$01.00

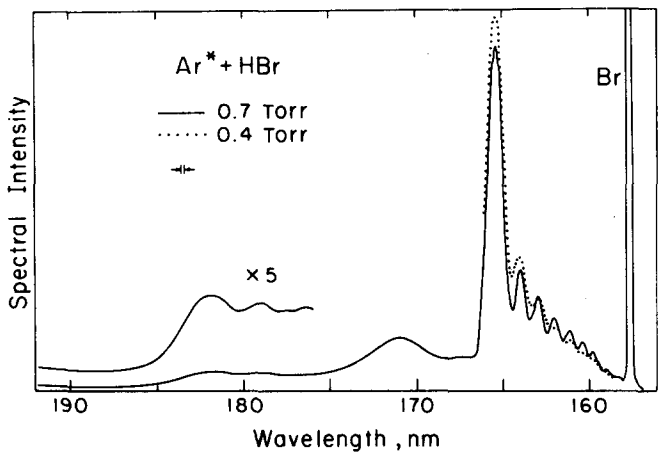

FIG. 1. Chemiluminescence spectrum of the reaction of $Ar^*(^3P_{0,2})$ with HBr. The high- and low-pressure spectra are normalized to constant Br-line intensity. Monochromator spectral resolution: 0.2 nm.

continua at longer wavelengths. Intensities in the ArBr $B-X$ continuum (158–166 nm) were corrected for weak scattered light associated with the Br lines; for CH_2Br_2 and HBr as reagents, this correction amounted to respectively approximately 13% and 6% of the total signal at 160 nm and 2% and 0.6% at 165 nm. For detailed studies of the $C-A$ and $B-A$ continua at longer wavelengths, a spectrosil window was inserted in the optical path, effectively eliminating the Br lines, while leaving these continua unaffected.

All spectra presented in this paper have been corrected for the spectral response of the detection systems[12] and are displayed with emission intensities proportional to quanta per wavelength interval. The spectra have been smoothed to remove the statistical noise in the original spectra, which was typically 5% of the signal for the weakest portions of the $B-X$ and $B-A$ continua and less than 2% of the signal otherwise.

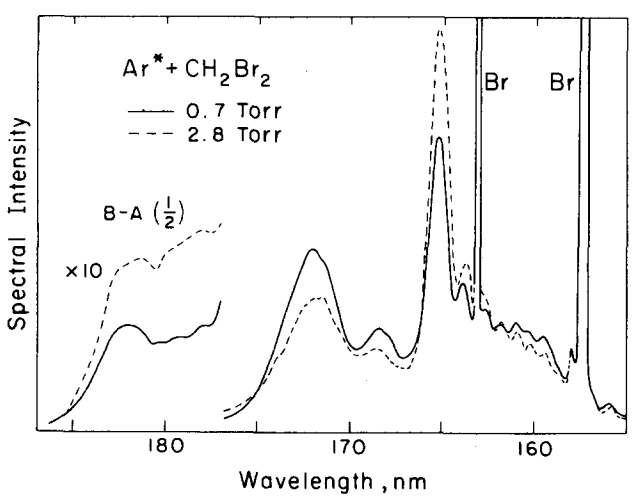

FIG. 2. Chemiluminescence spectrum of the reaction of $Ar^*(^3P_{0,2})$ with CH_2Br_2. The high- and low-pressure spectra are normalized to constant atomic Br emission intensity.

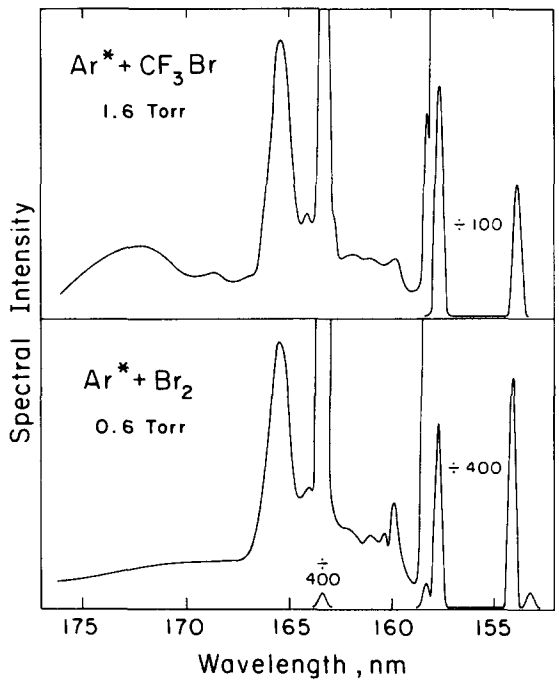

FIG. 3. Chemiluminescence spectra of the reactions of Ar* with CF_3Br and Br_2. The features at 160 nm include a grating ghost reflection associated with the Br line at 157.7 nm.

III. RESULTS

Spectra of the emission produced by the reactions of $Ar^*(^3P_{0,2})$ with various Br-containing compounds are shown in Figs. 1–3. Common to all the spectra are strong atomic Br lines, particularly those due to the transitions $4p^45s^{2,4}P_J-4p^5{}^2P_J$, and weaker continua, which extend from 157.7 nm, the wavelength of the $Br(^4P_{5/2}-{}^2P_{3/2})$ line, to long wavelength. By comparing the continua generated by these various reactions, three distinct regions of ArBr emission can be distinguished: the strongest "main continuum," extending from 158 to approximately 167 nm; a weaker "secondary continuum" between 167 and 176 nm; and a still weaker "third continuum" extending from 176 to 186 nm.

By analogy with other noble-gas halides,[8] the main continuum (MC) would be expected to be identified with the $B(\frac{1}{2})-X(\frac{1}{2})$ transition and the secondary continuum (SC) with the $C(\frac{3}{2})-A(\frac{3}{2})$ system (see the schematic potential curves, Fig. 4). In addition, we have recently shown[12] that the third continuum (TC) comprises the $B(\frac{1}{2})-A(\frac{1}{2})$ system.

Several spectra show further emission at longer wavelengths: sharply peaked structure in the $Ar^* + Br_2$ spectrum between 210 and 240 nm is probably due to Br_2^* emission, while a very weak continuum in the $Ar^* + HBr$ spectrum, which extends from 186 to beyond 300 nm, probably arises from emission of the HBr molecule.

The energetics of these reactions are clarified in Fig. 5. The reagent energy, available for formation of ArBr* or Br*, is the difference between the excitation energy of $Ar^*\ ^3P_2$ and the bond energy $D^0(R-Br)$ of the reagent molecule. The observed relative intensities of

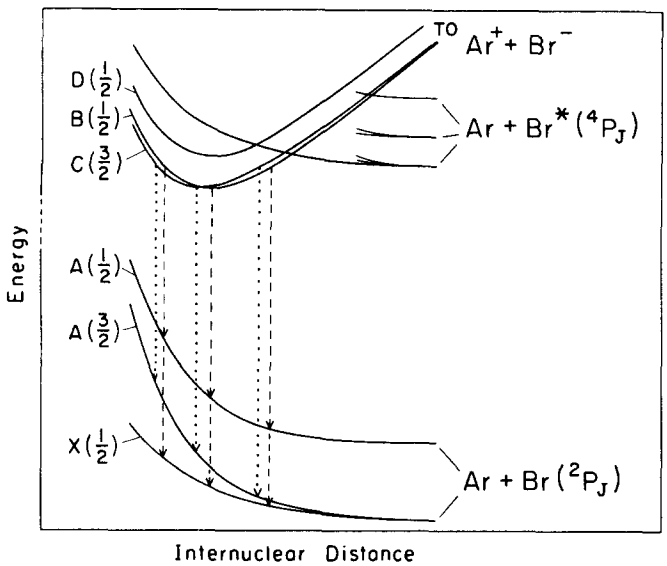

FIG. 4. Schematic potential curves of ArBr, with the transitions observed in this study. See Fig. 5 for the ordering of the Br spin–orbit levels.

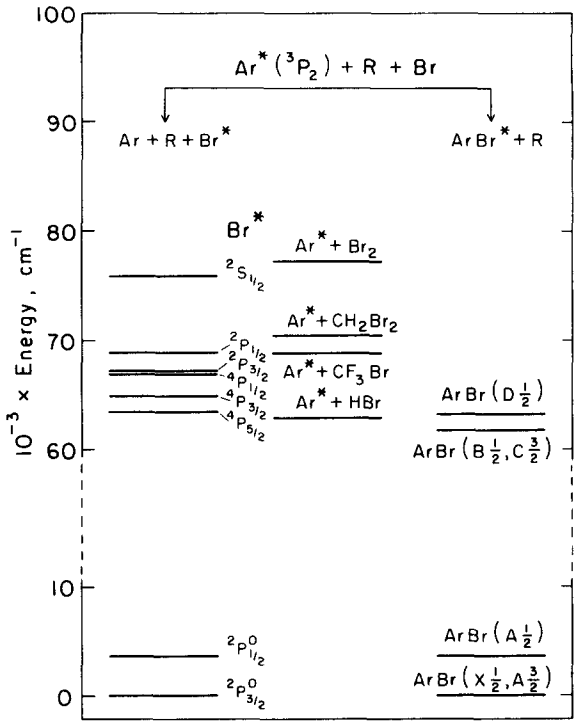

FIG. 5. Energy level diagram, illustrating the electronic states of ArBr and Br accessible in the reactions studied.

individual Br lines and ArBr emission are listed in Table I. For all reagents, Br* levels are populated up to the accessible limit, but ArBr emission is restricted essentially to vibronic states lying below these Br* levels. This clearly indicates that higher levels of the ArBr* states are predissociated to yield excited Br atoms.

Absolute intensities of ArBr emission decreased in the sequence of reagents: $HBr > CH_2Br_2 \sim Br_2 > CF_3Br > PBr_3$; thus, the first two reagents received the most study. A few experiments were also carried out with DBr.

The effect of total (Ar) pressure on the spectra was used to give information concerning the origin of the structure in the spectra. Over the pressure range 0.5–4 Torr, no significant change in the *relative* intensities of the Br lines was observed in any of the spectra. It can thus be concluded that the emitting levels are populated in the primary reaction step and that they suffer negligible quenching before emitting. The last conclusion follows from the very different radiative lifetimes of different levels[13]; if quenching occurred, it would be expected to affect different levels to a different extent. In the studies of the ArBr emission, therefore, the bromine line intensity was used as a measure of the extent of primary reaction of Ar* with RBr.

TABLE I. Relative intensities of spectral features resulting from the reactions of Ar* with RBr.

Bromine line	Wavelength (nm)	Relative intensity Br_2	PBr_3	CF_3Br	CH_2Br_2	HBr
$^2S_{1/2}-^2P^0_{1/2}$	138.5	7.3				
$-^2P^0_{3/2}$	131.8	12.9				
$^2P_{1/2}-^2P^0_{1/2}$	153.2	7.6	2.2	0.08	≤0.05	
$-^2P^0_{3/2}$	145.0	6.2	1.7	0.07	≤0.04	
$^2P_{3/2}-^2P^0_{3/2}$	148.9	23.4	18.2	4.1	0.4	
$^4P_{1/2}-^2P^0_{1/2}$	158.3	11.5	•••	0.7	≤0.05	
$^4P_{3/2}-^2P^0_{1/2}$	163.4	7.8	7.0	4.2	2.8	
$-^2P^0_{3/2}$	154.1	100	100	56	31.5	2
$^4P_{5/2}-^2P^0_{3/2}$	157.7	79.8	83.5	100	100	100
I_{Br^*}/I_{ArBr}		66	•••	15	5.2	1.8

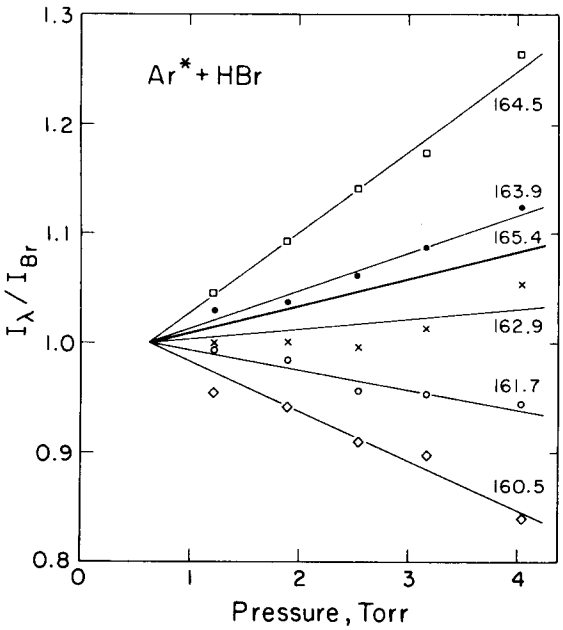

FIG. 6. Pressure dependence of emission intensity at selected wavelengths in the main continuum of Ar* + HBr. Ordinate: ratio of ArBr emission intensity to that of the 157.7 nm Br line. All data normalized to unity at 0.6 Torr.

The total integrated ArBr emission intensity varied little relative to the Br line intensity with pressure, but the three continua showed large changes relative to each other. The most marked behavior is shown in the Ar* + CH_2Br_2 spectrum (Fig. 2), where the SC (C–A system) is seen to weaken sharply with increasing pressure while the MC (B–X) and TC (B–A) strengthen proportionately. Analogous behavior was seen in the other

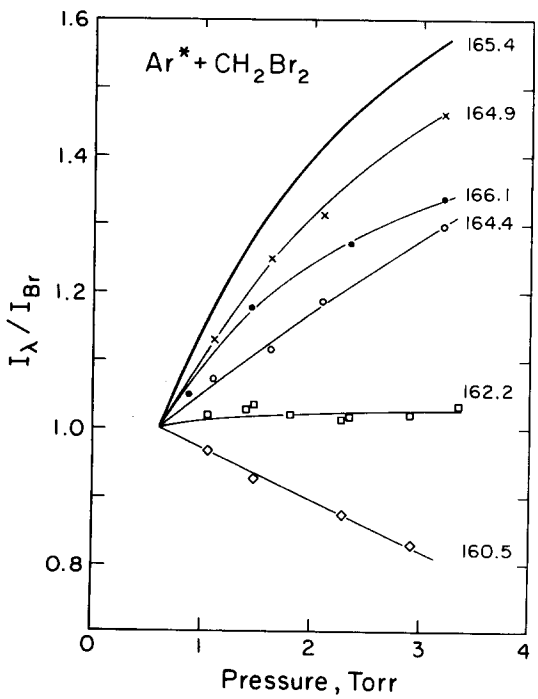

FIG. 7. Pressure dependence of emission intensity at selected wavelengths in the main continuum of Ar* + CH_2Br_2. See caption to Fig. 6 for details.

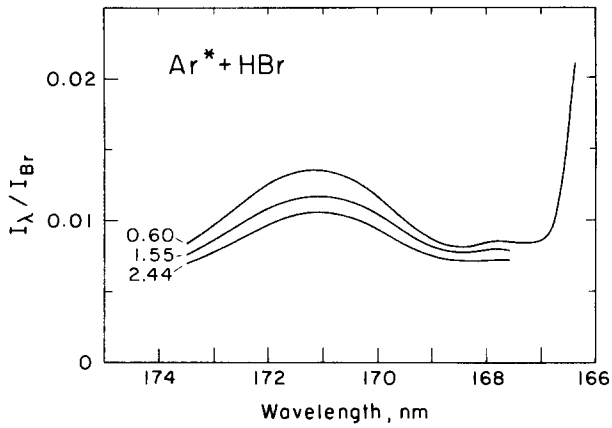

FIG. 8. Pressure dependence of the secondary continuum of Ar* + HBr. Pressures given in Torr. Ordinate: Absolute ratio of ArBr emission intensity to that of the peak of the 157.7 nm Br line. Monochromator spectral resolution: 0.4 nm.

systems; all the data were consistent with collisional quenching of C state molecules to the B state as the dominant electronic quenching channel in this pressure range.

Variation in the pressure caused changes in the intensity distributions within the continua. The general trend is a shift of intensity to the long wavelength end of the MC with increasing pressure and to short wavelength for the C–A and B–A continua. Several individual continua are treated in more detail below.

A. Ar* + HBr main continuum

The peak at 165.4 nm varied little in intensity relative to the Br line intensity, an increase of between 5% and 10% being found between 0.6 and 4 Torr (Fig. 1). The pressure dependences at other wavelengths in the MC are shown in Fig. 6, the intensity ratio being normalized to unity at 0.6 Torr. As expected, the general trend is a shift of intensity to long wavelength as the pressure increases. However, the greatest positive pressure dependence is not at 165.4 nm but in the region 164.4–164.7 nm, which corresponds to the first trough in the oscillatory structure.

B. Ar* + CH_2Br_2 main continuum

The pressure dependence, Fig. 7, differs markedly from that for HBr. The peak at 165.4 nm shows the greatest effect of pressure and increases, relative to the Br line intensity, by more than 50% over the pressure range 0.6–3 Torr. The region around 164.4 nm shows a much smaller positive pressure dependence while, below about 162 nm, an inverse pressure dependence is exhibited. The oscillatory structure, which is much less pronounced than in the Ar* + HBr spectrum, is not greatly affected by this pressure change.

C. Ar* + HBr, CH_2Br_2 secondary continua

Spectra of the SC region at several pressures are shown in Figs. 8 and 9. Both spectra show very similar behavior; strong quenching of the regions of maximum intensity and much weaker quenching of the troughs.

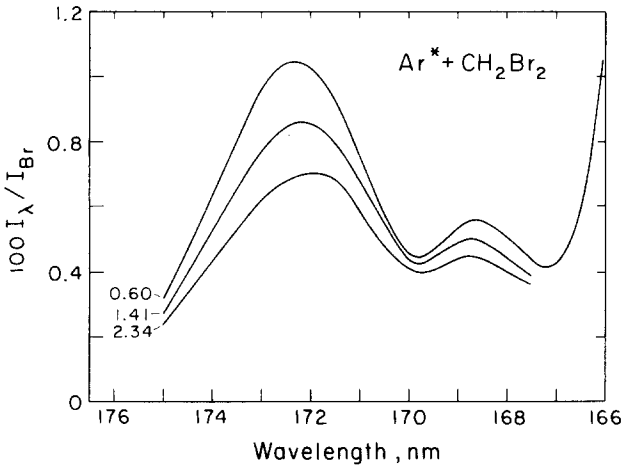

FIG. 9. Pressure dependence of the secondary continuum of $Ar^* + CH_2Br_2$. See caption to Fig. 8 for details.

The shift in the SC maximum with pressure is most evident in the $Ar^* + CH_2Br_2$ spectrum; however, even at high pressure, the peak, at 172.0 nm, is still definitely to long wavelength of that in the $Ar^* + HBr$ spectrum (171.0 nm).

The effect of temperature changes on the $Ar^* + HBr$ spectrum was investigated by surrounding the observation vessel with dry ice, which lowered the gas temperature in the reaction zone to about 240 K. The principal effects of the lowering in temperature were a small (5%–10%) rise in the absolute intensity of the MC peak at 165.4 nm and of the *B–A* continuum, but a lowering of the intensity of most of the rest of the spectrum. In the SC, all the wavelengths monitored, 167.7, 169, 171, and 173 nm, showed essentially the same decrease, 19% ±1%, relative to the MC peak. In the MC, in contrast, the lowering varied with wavelength, the results of several experiments being summarized in Table II; only below 160 nm did the temperature dependence become large, the Br line at 157.7 nm weakening by nearly 40% relative to the MC peak.

IV. DISCUSSION

A. Formation of Br* and ArBr*

The study of reactions of excited noble-gas atoms, A*, with halogen-containing compounds, RX, has now spanned almost all combinations of Ar, Kr, and Xe with F, Cl, Br, and I.[8,12,14,15] With the exception of ArCl, ArBr, ArI, KrI, and XeI, the continuous emission extends to a low wavelength limit, consistent with conversion of the entire exothermicity of reaction into vibronic energy of the noble-gas halide in at least a small fraction of the reactive encounters. In the above exceptional cases, atomic halogen lines may cut off the AX* continua before this low wavelength limit, through predissociation of the molecular emitting states

$$A^* + RX \rightarrow AX^* + R \ , \tag{1}$$

$$AX^* \rightarrow A + X^* \ , \tag{2}$$

$$X^* \rightarrow X + h\nu \ . \tag{3}$$

For ArCl and XeI, only very high vibrational levels are predissociated and atomic emission is seen only when reagents with weak R–X bonds, such as Cl_2 or I_2, are used. For ArBr and KrI, the predissociation occurs at very low vibrational quantum numbers and it is rather difficult, especially in the case of KrI,[12] to observe the unpredissociated levels. In the extreme case of ArI, I* levels lie below the minimum of the expected ionic ArI* state and it appears that *all* vibrational levels are predissociated: the spectra show no evidence of continuous emission in the region of the atomic I lines.

In discussing the reactions of the excited noble-gas atoms (A*) with halogen-containing molecules, the analogy with alkali atom (M) reactions[16,17] has proved very powerful. It has been suggested[8,10] that for reaction with a given RX, the vibrational distributions in the analogous AX* and MX states are comparable. It is therefore interesting to consider whether the combination of atomic Br and continuous ArBr emission from the $Ar^* + RBr$ reactions form an intensity distribution that can be compared with the vibrational distributions in KBr from $K + RBr$ reactions[16,17] (no predissociation occurs in this case, of course). In attempting such a comparison, it must be noted that not all the Br* emission need arise from predissociation of ArBr*; an alternative energy transfer mechanism is always possible:

$$Ar^* + RBr \rightarrow Ar + RBr^* \ , \tag{4}$$

$$RBr^* \rightarrow R + Br^* \ . \tag{5}$$

For $RBr = Br_2$, it seems unlikely that this energy transfer channel is important by analogy with the reactions of other A^*/X_2 pairs, in which the atom transfer reaction (1) is the dominant channel.[14,15] As the Br* intensity distributions from the reactions of Ar* with PBr_3, CF_3Br, and CH_2Br_2 show features in common with that from $Ar^* + Br_2$ (see Table I), it is probable that for these too the energy transfer channel is not dominant.

As shown in Table I, the spectra of $Ar^* + Br_2$ and PBr_3 show the distributions most shifted to high energies, both among the Br* levels and in the weakness of the ArBr emission. CF_3Br and CH_2Br_2 in that order show increasing shifts of the distribution to low energies.

TABLE II. Temperature dependence of the Ar* + HBr main continuum. Percent reduction, Δ, in $I_\lambda/I_{165.4}$ on cooling from 295 to 240 K.

Wavelength (nm)	Spectral feature	$\Delta(I_\lambda/I_{165.4})\%$
164.4	Trough	+1±1
164.0	Peak	−1±1
163.4	T	−1±1
162.9	P	−3.7
162.4	T	−5.5
162.0	P	−4.3
161.1	P	−4.9
160.4	P	−6.4
159.8	P	−11±1
159.0	P	−19±2
157.7	Br line	−37±2

Consistent with this behavior, Br_2 and PBr_3 are known to react with K atoms via a "direct" mechanism, in which relatively little energy of reaction appears as translation of the product,[16] whereas considerable translational energy release is observed in the reactions of alkali atoms with CH_2Br_2.[18] CF_3Br probably reacts similarly to CF_3I[19] and thus occupies an intermediate position. The present finding for CF_3Br and CH_2Br_2 is especially significant in that CF_3Br has a larger bond energy, $D^0(R-Br)$, than CH_2Br_2 (see Fig. 5).

The observed Br* distributions are surprising: firstly, in showing very weak emission from the $^4P_{1/2}$ level and, secondly, in the finding that the lowest levels $^4P_{5/2}$ and $^4P_{3/2}$ have the strongest populations, even in the strongly exothermic reactions with Br_2 and PBr_3. While the former effect partly reflects the different numbers of predissociating states, which correlate with each excited atomic state and possible differences in the strengths of the coupling of these states with the ionic states, these considerations can not explain the observation that the weakness of $^4P_{1/2}$ emission relative to that from $^2P_{3/2}$ is most marked in the least exothermic reactions, those of Ar* with CF_3Br and CH_2Br_2. As the $^4P_{1/2}$ level lies only 300 cm^{-1} below the $^2P_{3/2}$ level, we propose that the molecular $\Omega=\frac{1}{2}$ ($^4\Sigma^-$) state, which correlates with Ar + Br ($^4P_{1/2}$), is strongly repulsive and lies above molecular states correlating with $^2P_{3/2}$ in the region where these states cross the ionic B and C states. In this case, the low intensity of $^4P_{1/2}$ emission reflects the low population of the ionic states at high energies which can be predissociated by the $^4\Sigma^-$ ($\Omega=\frac{1}{2}$) state. In the reaction with Br_2, higher energies are available and the $^4P_{1/2}$ level is somewhat more efficiently populated. This explanation is supported by our recent finding[20] that the $^4P_{1/2}$ level in the CF_3Br reaction is, in fact, largely populated by reaction with the more energetic Ar* $^3P_0$ metastable, which is a minor species in our system.

The high populations of the $^4P_{5/2}$ and $^4P_{3/2}$ levels in the reaction with Br_2 are less easy to understand. The schematic potential curves in Fig. 4 show crossings of the ionic and predissociating states only at low energies, whereas, by analogy with K + Br_2, the reaction of Ar* + Br_2 would be expected to populate ArBr* initially at much higher energies. These conditions should not favor predissociation by the lowest-lying states, as the relative velocity of the atoms in this region is near its maximum. No crossing on the inner limb of the ionic curves has been shown as this would require the states correlating with Ar + Br* to be significantly less repulsive than the ionic states at small internuclear distances. As discussed in the following paper, the states correlating with *ground-state* Br + Ar are as repulsive as or more repulsive than the ionic states, and there are no low-lying molecular Rydberg states with which Ar + Br* ($^4P_{5/2,3/2}$) can correlate.

A possible solution to this problem is predissociation *during* the Ar* + Br_2 encounter. This could occur by a further electron jump in the $Ar^+Br_2^-$ intermediate to yield Br_2 in highly excited ionic states, Br^+Br^-. The ionic states lying in the appropriate energy range are those correlating diabatically with Br^+ (^1D, ^1S) + Br^- (^1S); these ionic products are not accessible energetically and adiabatic dissociation to the neutral atoms, Br* (^4P, ^2P) + Br ($^2P^0$), would result. The efficient formation of the lowest levels Br ($^4P_{5/2,3/2}$) would then reflect the detailed interactions between the ionic and covalent states of Br_2 or may arise because the departing Ar atom carries considerable kinetic energy.

B. Analysis of the ArBr continua

The major aim of this paper is to establish that the kinetic and spectroscopic data presented here allow an unequivocal assignment of the spectra and a complete understanding of the changes in the spectra with reagent, pressure, and temperature. This is an essential prerequisite of meaningful simulations of the spectra, which are described in the following paper. The present discussion concentrates mainly on the spectra generated by the reactions of Ar* with CH_2Br_2 and HBr; the data for the other reagents are consistent with these.

The spectra presented in Sec. III have been explained in terms of three transitions of ArBr: $B(\frac{1}{2})$–$X(\frac{1}{2})$, $B(\frac{1}{2})$–$A(\frac{1}{2})$, and $C(\frac{3}{2})$–$A(\frac{3}{2})$. In the spectra of several noble-gas halides, the $D(\frac{1}{2})$–$X(\frac{1}{2})$ system has been observed weakly.[15] The absence of such emission in ArBr is consistent with predissociation of the entire D state, which is expected to lie approximately 1400 cm^{-1} above the B state.

The form of the Ar* + HBr main continuum, which exhibits at least eight distinct peaks, indicates that the levels $v'=0$–7 of the B state are contributing to the spectrum. The strong peak at 165.4 nm cannot be ascribed wholly to emission from $v'=0$; rather, this continuum is analogous to the MC of other noble-gas halides,[8–10] in which the strong emission at long wavelength contains contributions from all emitting vibrational levels. This is characteristic of the situation in which the lower state (X) potential curve is no steeper than the repulsive limb of the upper (B) potential. This conclusion is supported by the pressure dependence of this continuum (Fig. 6), in which the greatest positive pressure dependence occurs to low wavelength of the strong peak. As shown in Paper II, it is that region which is dominated by emission from $v'=0$. The effect of pressure is therefore consistent with a shift of the vibrational distribution to low levels as the pressure increases, as expected if vibrational relaxation is dominant.

In order to understand the great difference between the MC of the Ar* + HBr and CH_2Br_2 reactions, it is necessary to examine the secondary continua. In both cases, these exhibit broader oscillations than the MC, extend to long wavelength of the MC peak, and shift, with increase in pressure, to low wavelength. This is characteristic of a transition, in which the lower $A(\frac{3}{2})$ potential curve is steeper than the repulsive limb of the upper C potential and the finding that the CH_2Br_2 spectrum extends further to long wavelength than does the HBr spectrum implies that higher vibrational levels are populated in the former case.

The potential curves, Fig. 4, show that the $B-X$ and $C-A(\frac{3}{2})$ continua should have closely similar low wavelength thresholds, close to the Br line at 157.7 nm, so that the MC must contain contributions from both transitions. In the $Ar^* + HBr$ spectrum, where the SC is very weak (Fig. 1), the $C-A$ contribution to the MC is probably small but in $Ar^* + CH_2Br_2$, where the SC is extremely strong, this contribution cannot be ignored and is almost certainly the reason for the more complex form of the MC in this case (Fig. 2).

The effect of increased pressure on the form of the MC of $Ar^* + CH_2Br_2$, namely, a dramatic strengthening of the long wavelength peak, is due to a combination of three possible effects.

(i) vibrational relaxation in the B state;

(ii) enhancement of the B state population by collisional crossing from the C state;

(iii) collisional depletion of the underlying $C-A(\frac{3}{2})$ emission.

As the 165.4 nm peak includes emission from all emitting vibrational levels, neither (i) nor (ii) alone can explain this phenomenon. As effect (i) can be no more pronounced than in the HBr spectrum, we conclude that both (ii) and (iii) are important factors: near 165.4 nm, the enhancement of the B state emission is dominant, whereas around 160 nm, depletion of the underlying $C-A$ emission is more important. Near 162 nm, both effects occur and annul each other over the pressure range investigated. In contrast, in the $B-A(\frac{1}{2})$ continuum, (ii) is dominant and the whole continuum is strongly enhanced by increase of pressure (see Fig. 2).

From the experimental evidence alone, it is not possible to assess how greatly the vibrational distribution in the B state is changing with pressure. Preliminary calculations suggest that the pressure increase from 0.5 to 4 Torr causes a very small shift to lower levels. This implies that collisional crossing between the C and B states involves several vibrational levels of both states.

The effect of pressure on the secondary continuum is shown in Figs. 8 and 9 for $Ar^* + HBr$ and CH_2Br_2. For these reagents and also for Br_2 and DBr, increased pressure causes a modest shift of intensity to low wave lengths and a diminution of the oscillatory structure, as well as of the overall intensity. Thus, the peaks in the SC are quenched more rapidly than the troughs and the long wavelength sides of the peaks more rapidly than the low wavelength sides.

In discussing this effect, it is again necessary to consider the composition of the SC, comprised principally of $C-A(\frac{3}{2})$ emission but with underlying $B-A(\frac{1}{2})$ emission. From the potential curves (Fig. 4), the low wavelength threshold of the latter continuum is expected to be shifted relative to that of the $B-X$ system by the spin–orbit splitting of the Br atom, to a wavelength of 167.5 nm. It is expected that the $B-A(\frac{1}{2})$ continuum shows a steadily decreasing intensity (except for broad oscillations) between the exposed portion and this wavelength, with an increase in intensity as the pressure is increased.

The overall reduction in the SC intensity with increased pressure is undoubtedly due to electronic quenching of the C state to the B state but the change in shape could again be due to several factors:

(i) different rates of electronic quenching for different vibrational levels of the C state;

(ii) vibrational relaxation within the C state;

(iii) enhancement of the underlying $B-A(\frac{1}{2})$ continuum.

Model calculations were carried out to simulate the observed changes in the $Ar^* + CH_2Br_2$ continuum on the assumption that only (iii) was responsible. These required the underlying $B-A(\frac{1}{2})$ emission to be unreasonably strong, with intensity maxima corresponding to the minima in the SC and strong emission also in the region 167–8 nm, where neither $B-X$ nor $B-A(\frac{1}{2})$ can contribute strongly.

Therefore, the changes in the SC reflect changes in the vibrational distribution of the C state. The computer simulations, presented in Paper II, show large pressure effects in the C state distribution, with possible enhancement of the lowest levels at high pressure, a clear indication that vibrational relaxation within this state is important.

The efficiency of electronic quenching of the C state to the B state can be estimated from the pressure dependence of the total SC, relative to the intensity of atomic Br emission. For $Ar^* + CH_2Br_2$, for which the effect of the $B-A$ emission is weakest, the integrated intensity I_{tot} between 167.5 and 175 nm gives an approximately linear Stern–Volmer plot of $1/I_{tot}$ against pressure, yielding a half-quenching pressure of 5 ± 1 Torr. An analogous analysis of the $Ar^* + HBr$ SC, with correction for underlying $B-A$ emission, yields a similar value. If the radiative lifetime of the C state is taken as 100 ± 50 ns, by analogy with *ab initio* calculations on several noble-gas halides,[21,22] the electronic quenching rate constant for Ar as collision partner is derived as $(6^{+6}_{-2}) \times 10^{-11}$ cm^3 s^{-1}. The rate constant for vibrational relaxation is probably at least as large.

C. Absolute energy of the $B(\frac{1}{2})$ state

As is shown in Paper II, comparison of simulated and experimental spectra, especially of the $Ar^* + HBr$ MC, provides reliable information on the relative shapes of the upper (B) and lower (X) potential curves. However, the absolute positions are less certain, as the spectrum probes these potentials only over a limited range of internuclear distance and these regions of the potentials could be raised or lowered by up to several hundred wave numbers while still maintaining reasonable overall shapes for the potential curves.

Insight into the absolute excitation energy (T_e) of the minimum of the B state potential curve is obtained from the temperature dependence of the $Ar^* + HBr$ spectrum. Because of the large bond energy of HBr, 86.5 ± 0.3 kcal mol^{-1},[23] only 62 900 cm^{-1} of energy (at 0 K) is available in this reaction for formation of ArBr* or Br*, which corresponds to a wavelength threshold in the spectrum of 159.1 nm. Thus, formation of $Br^*\ ^4P_{5/2}$ is

endothermic, whereas that of ArBr(B) is exothermic if the ground state is not too repulsive. If the temperature dependence of the Br line intensity is ascribed completely to the endothermicity of the formation process, a lowering of 48% of $I_{Br}/I_{165.4}$ on cooling the gas from 295 to 240 K is predicted, compared to the experimental value of 37% (Table II). The small difference is explained by the recent finding that at least 15% of Br* formation arises from the exothermic reaction of HBr with Ar* ($^3P_0$).[20]

For the ArBr MC, the absolute intensity of the peak at 165.4 nm is little affected by the temperature change, while the tail at low wavelength shows a negative temperature dependence (Table II). We propose therefore that low levels of the B state are populated exothermically and that the temperature dependence of a given high level relative to the low levels gives the degree of endothermicity for formation of the high level. Using the results of Paper II, we take the first trough at 164.4 nm to represent emission from low levels, as more than 90% of the emission at that wavelength derives from $v' = 0$ or 1.

For $v' = 7$, emitting at 159.0 nm, the 20% drop in $I_{159}/I_{164.4}$ between 295 and 240 K implies an endothermicity of ~ 200 cm^{-1}. The temperature dependence for $v' = 7$ may be slightly underestimated because of a small extent of formation of this level by the exothermic reaction of Ar($^3P_0$) with HBr. As the vibration frequency in ArBr* is close to 200 cm^{-1} (Paper II), we conclude that levels $v' \leq 5$ are populated exothermically and, therefore, that $T_e \leq 61\,850$ cm^{-1} for the B state. The result is quoted as an upper limit as the temperature effect could arise from other causes; however, if T_e were larger, a larger temperature dependence is required. Data from the reaction of Ar* with DBr are consistent with this conclusion.

The calculations presented in Paper II lead to an estimate of a lower limit for T_e, $T_e \geq 61\,650$ cm^{-1}. Thus the absolute energy of the B state is defined as $61\,750 \pm 100$ cm^{-1}. It is interesting to note that the energy of the Br($^4P_{5/2}$) level thus corresponds to $v' = 8$ or 9 in the B state, so that these levels may not be predissociated. Weak emission can be observed to low wavelength of the last resolved peak at 158.9 nm in the MC of Ar* + HBr and CH_2Br_2 and probably reflects weak emission from these higher levels.

ACKNOWLEDGMENTS

We acknowledge the Donors of the Petroleum Research Fund, administered by the American Chemical Society, the Research Corporation, and the Royal Society for support of this research. The British Council is thanked for financial support for A. K.

[1] M. F. Golde and B. A. Thrush, Chem. Phys. Lett. **29**, 486 (1974).
[2] J. E. Velazco and D. W. Setser, J. Chem. Phys. **62**, 1990 (1975).
[3] M. F. Golde, "Gas Kinetics and Energy Transfer," Spec. Per. Rep. **21**, Chem. Soc., p. 121 (1976), Vol. 2.
[4] D. L. King and D. W. Setser, Ann. Rev. Phys. Chem. **27**, 407 (1976).
[5] C. H. Becker, P. Casavecchia, and Y. T. Lee, J. Chem. Phys. **69**, 2377 (1978); **70**, 2986 (1979).
[6] P. C. Tellinghuisen, J. Tellinghuisen, J. A. Coxon, J. E. Velazco, and D. W. Setser, J. Chem. Phys. **68**, 5187 (1978).
[7] A. Sur, A. K. Hui, and J. Tellinghuisen, J. Mol. Spectrosc. **74**, 465 (1979).
[8] M. F. Golde, J. Mol. Spectrosc. **58**, 261 (1975).
[9] J. Tellinghuisen, A. K. Hays, J. M. Hoffman, and G. C. Tisone, J. Chem. Phys. **65**, 4473 (1976).
[10] K. Tamagake and D. W. Setser, J. Chem. Phys. **67**, 4370 (1977).
[11] P. J. Hay and T. H. Dunning, J. Chem. Phys. **66**, 1306 (1977).
[12] M. P. Casassa, M. F. Golde, and A. Kvaran, Chem. Phys. Lett. **59**, 51 (1978).
[13] G. M. Lawrence, Astrophys. J. **148**, 261 (1967).
[14] L. A. Gundel, D. W. Setser, M. A. A. Clyne, J. A. Coxon, and W. Nip, J. Chem. Phys. **64**, 4390 (1976).
[15] J. E. Velazco, J. H. Kolts, and D. W. Setser, J. Chem. Phys. **65**, 3468 (1976).
[16] J. L. Kinsey, in *Chemical Kinetics*, M. T. P. International Review of Science, edited by J. C. Polanyi (Butterworths, London, 1972), Vol. 9, p. 173.
[17] D. R. Herschbach, Adv. Chem. Phys. **10**, 319 (1966).
[18] E. A. Entemann, J. Chem. Phys. **55**, 4872 (1971).
[19] P. R. Brooks, J. Chem. Soc. Faraday Discuss. **55**, 299 (1973).
[20] M. F. Golde and G. W. Prohaska (unpublished results).
[21] T. H. Dunning and P. J. Hay, J. Chem. Phys. **69**, 134 (1978).
[22] P. J. Hay and T. H. Dunning, J. Chem. Phys. **69**, 2209 (1978).
[23] (a) *JANAF Thermochemical Tables*, Natl. Stand. Ref. Data. Ser. Natl. Bur. Stand. **37**, (1971), 2nd ed; (b) *Handbook of Chemistry and Physics* (Chemical Rubber, Cleveland, OH, 1975), 55th ed.